Toward a Better Understanding of Steric Stabilization When Using Block Copolymers as Stabilizers of Single-Walled Carbon Nanotubes (SWCNTs) Aqueous Dispersions

ARTICLE *in* MACROMOLECULES · SEPTEMBER 2012

Impact Factor: 5.8 · DOI: 10.1021/ma301534k

3 AUTHORS:

Antonello Di Crescenzo
Università degli Studi G. d'Annunzio Chieti e P…
15 PUBLICATIONS **166** CITATIONS
SEE PROFILE

Massimiliano Aschi
Università degli Studi dell'Aquila
171 PUBLICATIONS **2,755** CITATIONS
SEE PROFILE

Antonella Fontana
Università degli Studi G. d'Annunzio Chieti e P…
99 PUBLICATIONS **1,020** CITATIONS
SEE PROFILE

Macromolecules

Article

pubs.acs.org/Macromolecules

Toward a Better Understanding of Steric Stabilization When Using Block Copolymers as Stabilizers of Single-Walled Carbon Nanotubes (SWCNTs) Aqueous Dispersions

Antonello Di Crescenzo,[†] Massimiliano Aschi,[‡,*] and Antonella Fontana[†]

[†]Dipartimento di Farmacia, Università "G. d'Annunzio", Via dei Vestini, I-66100 Chieti, Italy

[‡]Dipartimento Scienze Fisiche e Chimiche, Università degli Studi di L'Aquila, Via Vetoio (Coppito 1), I-67010 L'Aquila, Italy

Supporting Information

ABSTRACT: Starting from experimental evidence of the goodness of poly(ethylene glycol-*bl*-propylene sulfide), PEG–PPS, to disperse single-walled carbon nanotubes (SWCNTs), atomistic molecular dynamics (MD) simulations have been performed to study SWCNTs/polymer systems in the presence of water molecules in solution. Comparison between block copolymer (PEG–PPS) and homopolymer (PEG) and between single and double chains system is presented. Results show that the hydrophobic nature of PPS systematically ensures a higher SWCNT surface coverage, a higher interstitial water depletion and a much lower degree of water ordering when compared to the PEG homopolymer.

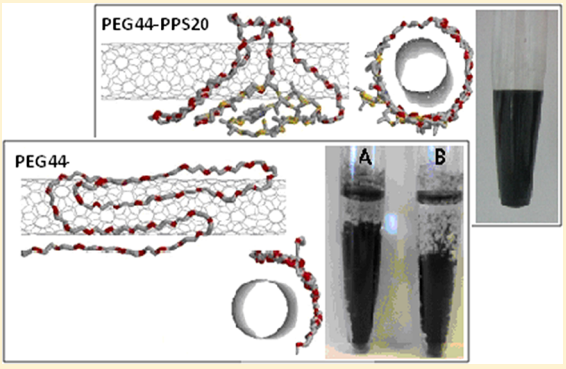

1. INTRODUCTION

Single-walled carbon nanotubes (SWCNTs) are tubular forms of carbon that can be envisaged as graphene sheets rolled into cylindrical form characterized by a high aspect ratio (ratio between length and diameter) having 0.3–2 nm of diameter and lengths up to 1 μm. They have unique mechanical, optical, and chemical properties, with broad potential biomedical applications, which include imaging, cancer therapeutics,[1−6] or cancer cells destruction.[7]

In the last years carbon nanotubes (CNTs) have been also widely used as in vitro delivery vehicles to effectively shuttle biomolecules[8,9] or drugs.[10,11] The main obstacles to their use as drug carriers are as follows: (a) their scarce solubility in any aqueous environment due to the graphitic nature of their sidewalls and (b) the need to elude, following administration, biological and biophysical barriers. Among those barriers, removal by the mononuclear phagocytic system, also known as the reticuloendothelial system (RES), can dramatically hamper the efficiency of a drug. To overcome these problems, we have previously modified[11,12] SWCNT surfaces by noncovalent coating SWCNTs with amphiphilic block copolymers, PEG–PPS, based on hydrophobic polysulfides (poly(propylene sulfide), PPS) and hydrophilic polyethers (poly(ethylene glycol), PEG). The good suspendability of SWCNTs induced by PEG–PPS was attributed[11,12] to the steric stabilization brought about by the anchoring of the hydrophobic domains to the SWCNT surface and the dangling into the solvent of the highly hydrophilic and flexible PEG chains,[13,14] that ensures minimization either of the interactions leading to sequestration in the RES organs[15] and van der Waals interactions between carbon nanotubes. Solvent selectivity is the driving force for the above-mentioned effect[15] because the poor solvated block adsorbs,[16] onto the colloid concentrating at its surface in order to minimize contact with the solvent, whereas the well solvated block readily increases its spatial dimensions and reduces its configurational entropy in order to maximize its degree of solvation.

According to previously published evidence[12] also the presence of PEG seems to be crucial for enhancing the solubilizing and dispersing activity toward SWCNTs. These results have stimulated our curiosity in order to better understand and rationalize as to what are the major determinants at the basis of the mechanism of SWCNTs solubilization and, in particular, solvated SWCNTs stabilization.

In this study we have addressed this latter question. The initial problem to face is the choice of a suitable theoretical-computational viewpoint.

In fact, the possibility of solubilizing SWCNTs, utilizing specific molecular or macromolecular systems relies on the combination of many competing processes supposed to act at different energy and time scales.[17] Hence, even neglecting local chemical effects,[18] a wide repertoire of subtle physical determinants ranging from the local weak nonbonding interactions to the collective thermal and entropic effects are expected to play a role.[19] Consequently, at the moment, does not exist any exhaustive computational-theoretical method and

Received: July 24, 2012
Revised: August 28, 2012
Published: September 28, 2012

an *a priori* selection of very narrow range of information does represent the strategy of whatever computational study in this field.

For example, quantum-chemical (QM) calculations, as recently demonstrated[20] are able to accurately quantify specific mechanical determinants (energies and forces) underlying the intimate interaction between solubilizers and SWCNTs but at the moment cannot properly take into account the complexity of the real system. This latter aspect can be partially addressed by the use of atomistic molecular dynamics (MD) simulations which, making use of empirical Hamiltonians, can describe thermal effects underlying semiclassical transitions with relaxation times of the order between picosecond and microsecond. In this time-regime, it has been possible to observe the effects occurring at the CNT, solute and solvent interface.[21−32] Slower events such as aggregation-disaggregation in solution, may be addressed only making use of less accurate but computationally more efficient coarse-grained Hamiltonians.[33−37]

In this study we have decided to utilize MD simulations for analyzing the interface between SWCNTs, polymer and water molecules in solution, by using the following strategy:

- We only consider the ensemble of already formed SWCNT-polymer aggregates (vide infra); i.e., no information is searched as far as the out-of-equilibrium aggregation process is concerned.
- Well aware of the limitations of the empirical force-fields for correctly describing local interaction effects governed by dispersion and polarization, and disregarding for the moment any systematic investigation concerning the performances of different force-fields, our study is based on the comparison between two different single-chains (SCs) molecular systems experimentally known to provide sharply different results: 10-mer of PEG (hereafter termed as PEG10) and a diblock copolymer of the same length including the polypropylene sulfide block (hereafter termed as PEG5−PPS5). Using this strategy we hope to reduce the inevitable systematic errors produced by force-field deficiencies by considering two parallel sets of simulations under perfectly identical conditions, i.e. same macromolecular lengths, same solvent density, same CNT dimension, same simulation protocol.

At this stage we have then pointed our attention to two further points: (i) effect of aggregation, by simulating both the above molecular systems in an aggregated fashion, and (ii) effect of molecular weight of the investigated polymers. Because of the complexity of the system we have simulated the simplest "aggregation state", which is the double chain (DC) fashion. These systems are hereafter termed as 2PEG10 and 2PEG5−PPS5.

Finally, the information obtained by the above ensemble of simulations have been exploited to study higher mass systems (i.e., the more realistic and experimentally investigated block copolymers) consisting of longer SCs: PEG44−PPS20 and PEG44.

2. EXPERIMENTAL SECTION

2.1. Experimental Details. *2.1.1. Materials.* Pristine HiPCO SWCNTs (lot #0556) were provided by Carbon Nanotechnologies, Inc. Houston, USA and were used as received. Poly(ethylene glycol) 200 (PEG4), poly(ethylene glycol) 1500 (PEG34), poly(ethylene glycol) 4000 (PEG90) were purchased from Alfa Aesar. Ultra pure Milli-Q water (Millipore Corp. model Direct-Q 3) with a resistivity of >18.2 MΩ cm was used to prepare all solutions.

2.1.2. Preparation of SWCNT Dispersions. The dispersions of SWCNTs were prepared by adding 5 mL of pure PEG or PEG aqueous solutions of different concentrations (2, 7, and >50 mg/mL) to 1 mg of pristine SWCNTs at 25 °C. The sample was then sonicated with an ultrasonic bath sonicator (Transsonic 310 Elma, 35 kHz) for 4 h. The obtained suspension was centrifuged for 10 min at 4000 rpm by using a Universal 32 (Hettich Zentrifugen) centrifuge in order to separate the supernatant aqueous solution from the precipitate.

2.2. Computational Details. The simulations in the presence of CNTs were initiated with the SCs or DCs located at a minimum distance 0.50 nm from the SWCNT which is kept frozen at the center of a box filled with water and the typical density at 298 K and 1.0 bar of pressure. The initial configuration utilized is the fully extended one. For DCs system, two chains both in the fully extended conformations were initially put in two opposite sides of CNT. In all the simulations, the dimensions of the boxes have been determined by ensuring absence of interaction between the replica of the polymer chains The dimension of the cubic box resulted equal to 281.0 nm^3. The simulations without SWCNT are carried out using exactly the same conditions. All the simulations were propagated for 80 ns (150 ns for the two longer chains) and the analyses (see below) have been carried out only when the chain−SWCNT minimum distance is not larger than 0.4 nm. Analyses in the presence of CNT have been performed by removing the translational (longitudinal) motion of the oligomer center of mass. For SWCNT standard Lennard-Jones parameters were utilized.[30] The geometry of the nanotube was generated by using the TUBE-VBS code.[38] A SWCNT with the following features was used: n = 10, m = 3, carbon−carbon distance of 0.1421 nm. No deformations were included.

The following protocol was utilized in all the simulations: the simulations were carried out in the canonical (NVT) ensemble, the systems were initially relaxed first mechanically (steepest descent), then dynamically by using 50.0 ps of short MD simulations from 50 to 300 K. After an equilibration of about 2.0 ns we performed the productive simulations of 80.0/150 ns using an integration step of 2.0 fs, the Berendsen temperature coupling.[39] The long-range electrostatics was treated by means of the particle mesh Ewald method.[40] The simulations were performed adopting the Gromacs software package.[41] Force field parameters for PEG were adapted from the literature[42] and inserted into the Gromos force-field.[43] The same force field was also utilized for PPS. The single point charge (spc) model[44] was adopted for water molecules. It is important to stress the fact that a systematic investigations on the performances of different force-fields on this kind of polymeric systems are still lacking in the literature, and hence, any *a priori* choice of whatever empirical Hamiltonian does induce unquantifiable systematic error in the final result.

3. RESULTS

3.1. Model Systems: Single and Double Chains of PEG10 and PEG5−PPS5. *3.1.1. Mechanical−Morphological Analysis.* It is first important to note that for all the simulated systems which we have initially focused on in this study, the SCs (i.e., PEG10, PEG5−PPS5) and DCs (i.e., 2PEG10 and 2PEG5−PPS5) maintain in the vicinity of CNT at an average minimum distance of 0.31 ± 0.01 nm (PEG10), 0.33 ± 0.06 nm (2PEG10), 0.33 ± 0.02 nm (PEG5−PPS5), and 0.35 ± 0.04 nm (2PEG5−PPS5). It means that, at least within the 80.0 ns of simulations, none of the SCs or DCs show a particularly reduced affinity toward SWCNT, i.e., a greater tendency to move away from the CNT. Some differences are found, on the other hand, analyzing the chain fluctuations. Results, whose details are reported in the Supporting Information (Figure S1) for the sake of brevity can summarized as follows:

- Much of the fluctuation of adsorbed DCs refers to interchains relative motions.

- The presence of PPS systematically confers a slightly higher rigidity to the DCs both in the adsorbed condition and in solution.
- Root mean square fluctuation (RMSF) of DC undergoes a slight reduction upon dispersion in water due to the formation of aggregates and consequent interchains relative motions reduction in agreement with the very low critical aggregation concentrations experimentally measured for similar polymers in aqueous solutions (see also the discussion below).[45,46,47]

The morphology of adsorbed SCs and DCs can be visualized by considering the chain conformations emerged from the simulations. Extraction of the statistical relevant conformations of the chains (and in general of any flexible species) is a very complicated task. In fact when we deal with a system characterized by a large number of internal degrees of freedom, the preselection of a subset of internal coordinates (e.g., the torsion angles in the peptide Ramachandran plots) can lead to biased and nonexhaustive results. To circumvent this difficulty we can utilize a well-assessed computational technique termed as essential dynamics (ED),[48] which is based on the redefinition of a subset of internal degrees of freedom directly from the simulation. This is accomplished by the construction and diagonalization of the atomic positional covariance matrix. Then the projection of the whole simulation onto this subset of essential coordinates can provide us with the desired conformations (see details of the method and Figures S2 and S3 in the Supporting Information). The results are reported in Figures 1 and 2 for the adsorbed SCs and DCs and, for comparison, in Figure 3 for the DCs in water without SWCNTs.

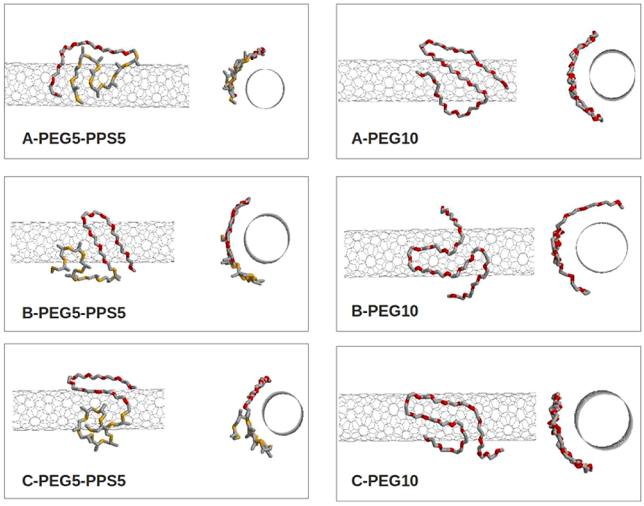

Figure 1. Representative structures (conformations) of PEG5−PPS5 and PEG10 adsorbed on SWCNT as obtained by essential dynamics analysis (see Supporting Information, Figures S2 and S3).

According to Figures 1 and 2, the presence of SWCNT heavily modifies the conformational repertoire of polymer chains. In line with previous studies,[49,50] all the chains tend to wrap SWCNT surface and the wrapping extension appears to sharply increase when going from SCs to DCs.[51] On the other hand both 2PEG10 and 2PEG5−PPS5 appear aggregated in water solution in agreement with the tendency of both PEG and PEG−PPS polymers to self-aggregate in water as recently emerged from experimental investigations for PEG12[45] and

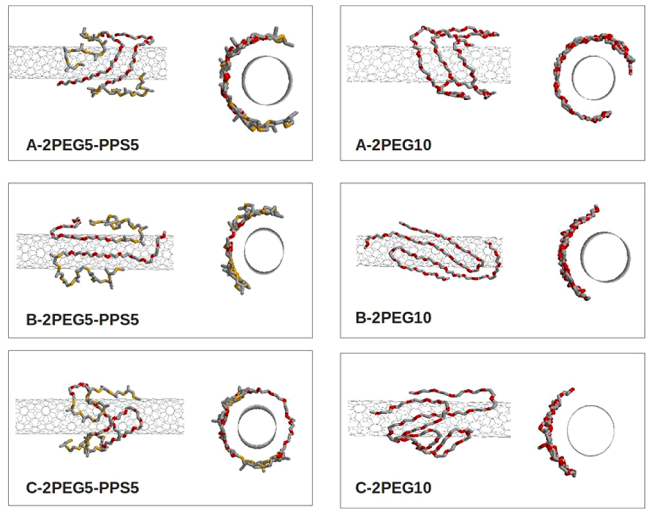

Figure 2. Representative structures (conformations) of 2PEG5−PPS5 and 2PEG10 adsorbed on SWCNT as obtained by essential dynamics analysis (see Supporting Information, Figures S2 and S3).

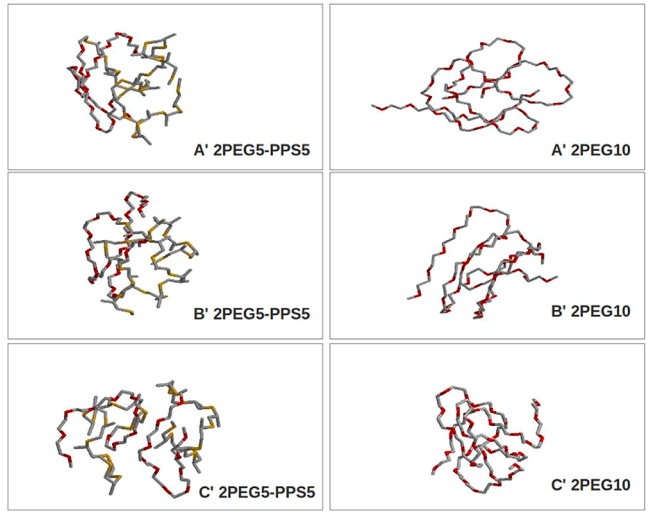

Figure 3. Representative structures (conformations) of 2PEG5−PPS5 and 2PEG10 in water solution as obtained by essential dynamics analysis (see Supporting Information Figures S2 and S3).

PEG17PPS38[47] and the reduced RMSF evidenced in solution (see comment in Figure S1 above).

In order to quantitatively appreciate the wrapping ability of the four systems emerged from Figures 1 and 2, we have calculated the wrapping Helmholtz free energy (ΔA_{wr})[23] defined as

$$\Delta A_{wr}(\Theta) = -RT \ln[P(\Theta)/P(\Theta_{ref})] \quad (1)$$

where Θ is the angle formed between the projections of two radial vectors passing through the terminal atoms i and j, projected onto the radial section of the nanotube (see inset of Figure 4), Θ_{ref} is the most sampled wrapping angle found along the simulation and $P(\Theta)$ and $P(\Theta_{ref})$ are the corresponding probabilities of occurrence along the simulations.

Low values of $\Delta A_{wr}(\Theta)$ in correspondence of low Θ values clearly indicate a high wrapping ability of the chain. From the Figures 1 and 2, SCs reveal as essentially unable to wrap the CNT. On the other hand DCs show a higher propensity to wrap SWCNTs but the fully wrapped condition ($\Theta = 0.0°$) is

dx.doi.org/10.1021/ma301534k | Macromolecules 2012, 45, 8043−8050

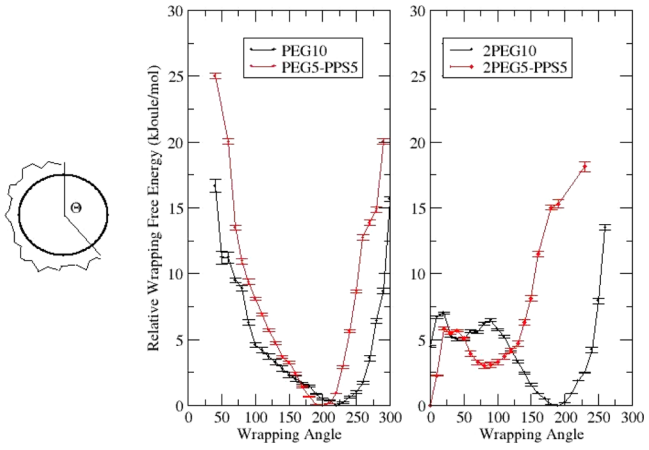

Figure 4. Relative wrapping Helmholtz free energy (eq 1) as a function of wrapping angle Θ (see inset) for the SC (left side) and DC (right side) systems. Error bars were estimated by considering three subportions of the whole trajectories. Note that angles not appearing in the graph were not sampled along the simulation and hence, for such angles, a virtually infinite relative wrapping free energy is attributed.

reached only in the case of 2PEG5−PPS5. Our findings suggest that wrapping ability depends on, at least, two variables: (i) presence of PPS moiety and (ii) relative dimension of CNT radius and polymer system.

To shed additional light on the morphological homologies and differences between the investigated systems, three additional observables have been taken into account: the radial probability of finding any type of atom belonging to the chains at different distances from the SWCNT surface (Figures 5 and 6), the longitudinal spread of the adsorbed polymer chains onto the SWCNT surface (Figure 7) and, finally, their coverage area with respect to the SWCNT surface (Figures 8).

From Figures 5 and 6, we do not observe appreciable differences in the thickness of adsorbed polymer between single and double chain. However it is worth noting that when the adsorbed systems, both SCs and DCs, contain the PPS domain

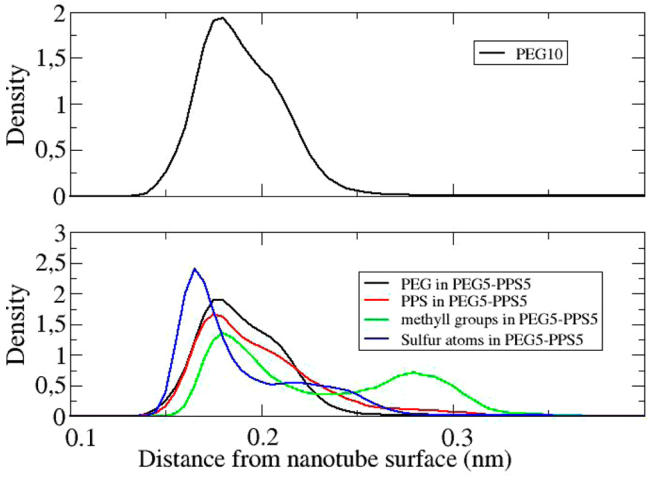

Figure 5. Probability density as a function of the radial distance from the SWCNT surface for PEG10 and PEG5−PPS5. The area of the different curves is equal to the number of the related species. Hence all the curves have been normalized for the sake of clarity. Values on the abscissa can be related to the radial thickness of the adsorbed polymer.

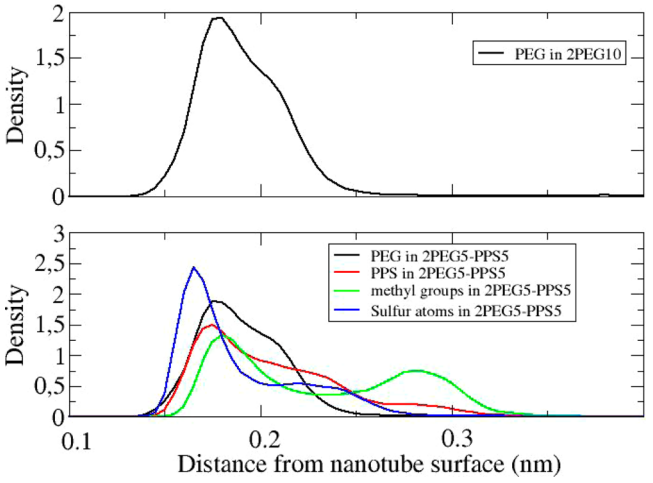

Figure 6. Probability density as a function of the radial distance from the SWCNT surface for 2PEG10 and 2PEG5−PPS5. In the upper panel the box highlights the region with a second local maximum in the probability density. The area of the different curves is equal to the number of the species the curves are referring to. Hence all the curves have been normalized for the sake of clarity. Values on the abscissa can be related to the radial thickness of the adsorbed polymer.

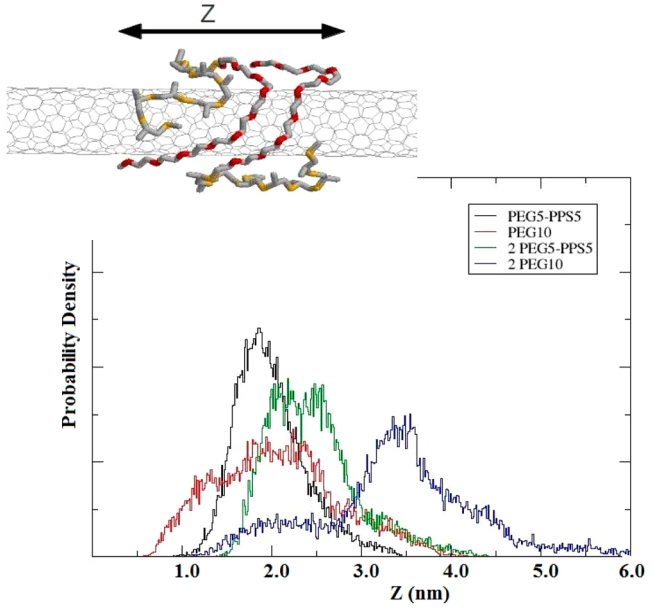

Figure 7. Normalized distribution of the maximum intrachain longitudinal (z) distance (see inset) spanned along the simulations for PEG5−PPS5 (black line), PEG10 (red line), 2PEG5−PPS5 (green line), and 2PEG10 (blue line). Values on the abscissa can be related to the longitudinal dimension of the adsorbed polymer.

their thickness (i.e., the maximum value of the abscissa) is systematically increased by more than 0.1 nm. Particularly interesting is the bimodal distribution shown by methyl groups and, although to a minor extent, by the sulfide groups. This behavior suggests a peculiar double role of these species consisting in both interacting with the hydrophobic SWCNT surface as well protruding toward the solvent.

Presence of PPS chain has also revealed to significantly, although not dramatically, affect the longitudinal spread of the different chains adsorbed on the SWCNT. This observable, as reported in Figure 7, can be defined as the chain longitudinal

dx.doi.org/10.1021/ma301534k | Macromolecules 2012, 45, 8043−8050

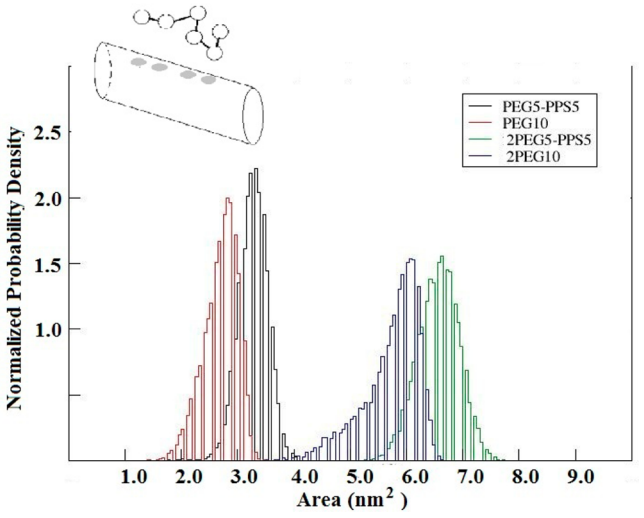

Figure 8. Normalized distribution of the coverage area evaluated along the simulations. In the inset is shown the schematic definition of the coverage-area utilized in this study.

dimension (the *z*-variable shown in the inset of the Figure) measured at each frame of MD.

The presence of PPS shifts the maximum of the distributions to lower values and also reduces their widths in SCs (compare red and black curves) as well as in DCs (compare blue and green ones) indicating that copolymers are, on average, longitudinally more compact. This latter effect, which will be found as amplified in the analysis of the large systems outlined in the next paragraph, is probably a consequence of the higher hydrophobicity of PPS moiety which tends to minimize the interaction with aqueous solvent. The two previous observables, i.e. the radial thickness of the adsorbed chains and their longitudinal coverage along the CNT surface, has inspired a last analysis, i.e. the measure of coverage area (CA) produced by the adsorbed species onto the SWCNT. For defining this quantity, whose result is reported in Figure 8, we refer to the scheme depicted in the inset of the same figure: CA is calculated at each MD frame as the sum of the projection of each atom (by considering the corresponding van der Waals radius) onto the SWCNT surface.

From the shape of the CA distributions in Figure 8 and their values of 6.57 ± 0.03 nm^2 (for 2PEG5−PPS5), 5.73 ± 0.05 nm^2 (for 2PEG10), 3.27 ± 0.03 nm^2 (for PEG5−PPS5) and 2.70 ± 0.02 nm^2 (for PEG10) we can infer that the presence of PPS ensures, both in SCs and DCs, a slight CA increase reaching its maximum in the case of 2PEG5−PPS5. Considering that *length* of the two set of chains is approximately the same, and also keeping in mind the results from the Figures 5−8, we may infer that the chain ability of covering the SWCNT surface depends on the chain molar mass increase, i.e., *density* increase, induced by the presence of methyl groups and sulfur atoms.

Combining the above findings we might schematically suggest that the investigated systems, although not showing different affinity toward the SWCNT surface, do interact with rather different patterns. In particular, the presence of PPS increases the radial thickness, the longitudinal compactness, allows a better wrapping to SWCNT and, finally, ensures a greater coverage of the SWCNT surface. Additional indications can be obtained by analyzing the role of the solvent.

3.1.2. Hydration Analysis. We have studied the degree of hydration of both the adsorbed species and the interface between the polymer and the SWCNT. The first information has been simply derived by evaluating the water pair correlation function, g(r), with respect to all the oxygen and sulfur atoms present in the investigated polymeric chains.

The results reported in Figure 9 clearly show a higher tendency of oxygen atoms to structure water molecules. This is

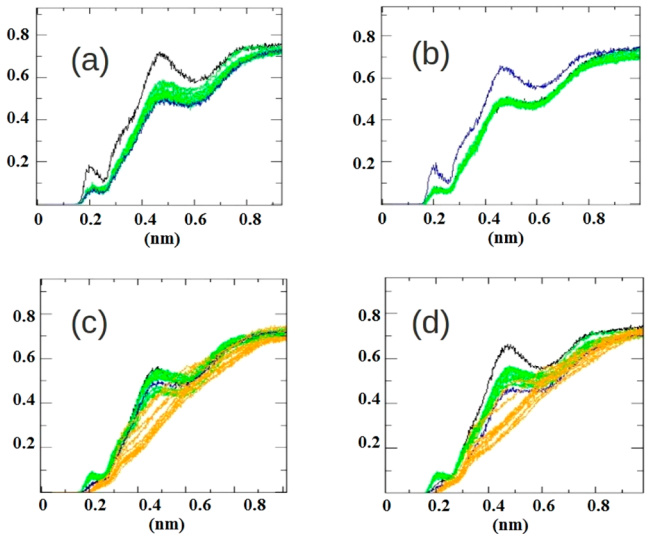

Figure 9. Water pair correlation function, g(r), evaluated with respect to PEG oxygen atoms (green curves) and PPS sulfur atoms (orange). Terminal oxygen atoms of the chains are reported in black and blue. Key: (a) first PEG in 2PEG10; (b) second PEG in 2PEG10; (c) first PEG5−PPS5 in 2PEG5PPS5; (d) second PEG5−PPS5 in 2PEG5−PPS5.

particularly enhanced in the case of PEG and in the case of terminal oxygen atoms. In correspondence of all the sulfide groups, although the solvent exposure is similar, we do not observe well-structured regions.

Worth of note is the fact that terminal oxygen atoms (black and blue curves) do not show a similar behavior in any of the investigated systems. This result reflects the geometrical asymmetry by the adsorbant already appreciated in the Figures 1−3.

Differential ability of PEG and PEG−PPS of inducing water structuration, certainly worth of deeper and more quantitative investigation in the future, allows us to qualitatively speculate about the thermodynamic role of the solvent in the formation of polymer-coated SWCNTs. Indeed adsorption of chains containing PPS moieties is probably not accompanied by the same loss of water configurational entropy shown by homopolymeric PEG chains characterized by a rather well-structured hydration shells.

This argument, somewhat speculative, might be however reinforced by considering the density of interstitial water, i.e. the accessibility of solvent molecules at the chain-nanotube interface. At this purpose, at each frame of the MD simulations, we have counted the number of water molecules whose projection onto the SWCNT surface overlaps with the chain projection (inset of Figure 8), and whose distance from SWCNT surface is lower than the distance of any atom belonging to the chain. Such a number of interstitial water molecules, whose distribution is reported in the Supporting Information for the four investigated systems (Figure S4) has been then divided by the instantaneous CA (Figure 8). The

dx.doi.org/10.1021/ma301534k | *Macromolecules* 2012, 45, 8043−8050

resulting superficial densities of interstitial water, equal to 1.7 ± 0.2 molecules/nm^2 (PEG10), 1.3 ± 0.1 molecules/nm^2 (PEG5−PPS5), 1.3 ± 0.2 molecules/nm^2 (2PEG10), and 0.5 ± 0.1 molecules/nm^2 (2PEG5−PPS5), clearly indicates that the increase of chain length but, most importantly, the presence of PPS strongly contributes to dehydrate the chain−CNT interface better than homopolymeric PEG does.

3.2. Real Systems: Single Chains of PEG44 and PEG44−PPS20. All the information learnt from the model systems has been exploited for analyzing the behavior of larger single-chains of PEG44 and PEG44−PPS20,[12] experimentally investigated as dispersing agent for SWCNTs. All the analyses previously shown have been repeated and the emerged picture confirms, and also reinforces, the peculiar role of PPS moiety. (See Supporting Information for the preliminary evaluation of RMSF and average minimum distances from the nanotube surface, Figure S5 and Table S1). This can be immediately visualized by the representative structures extracted with the same ED-based procedure followed for the model (See Supporting Information Figures S2 and S3) and reported in Figure 10. As a matter of fact, in this case, the presence of PPS

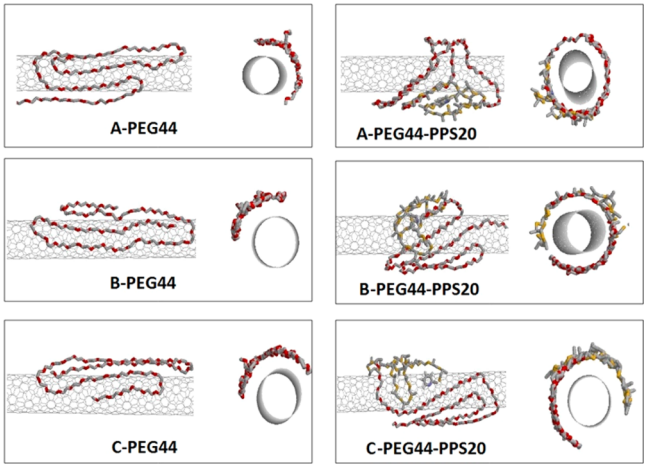

Figure 10. Representative structures of PEG44 and PEG44−PPS20 adsorbed on SWCNT as obtained by essential dynamics analysis (see Supporting Information Figures S2 and S3).

enables the chain to fully wrap the CNT. On the other hand, in the lack of PPS, the chain is longitudinally almost completely spread over the CNT surface.

This pictorial information can be more quantitatively appreciated by considering the results of the same analyses previously carried out for model systems and summarized in Figure 11. As expected, PEG44−PPS20 shows sharp absolute minimum of wrapping free-energy exactly corresponding to Θ = 0.0° whereas absence of PPS completely prevents the system to fully wrap the nanotube (Figure 11a). Consistently, the very peaked and narrow distribution of the longitudinal spread found for the homopolymeric PEG44 species, reported in Figure 11d, indicates that the absence of PPS keeps the chain spread over 4.30 ± 0.01 nm of the CNT (Figure 11d). Finally, the radial probability density function reported in Figures 11, parts b and c, and qualitatively similar to the results reported for the smaller systems in Figures 5 and 6, clearly shows that the tail of PEG44−PPS20 distribution (i.e., the maximum thickness) reaches values 0.10 nm higher than PEG44 homopolymer suggesting that the progressive increase in the dispersant

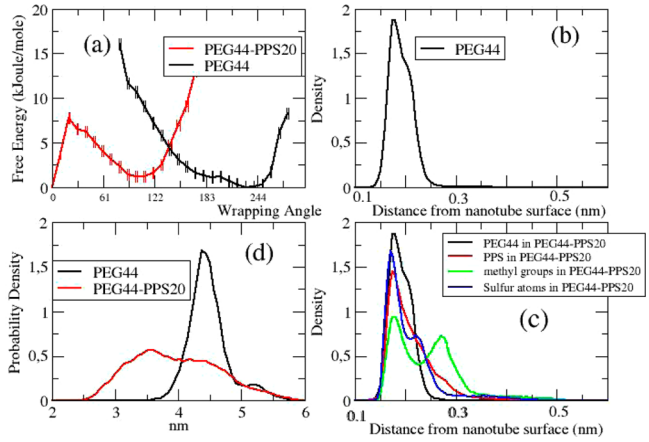

Figure 11. Inset a: relative wrapping free energy (for details, see the caption of Figure 4). Inset b: probability density as a function of the radial distance from the SWCNT surface for PEG44 (for details, see the caption of Figure 5). Inset c: probability density as a function of the radial distance from the SWCNT surface for PEG44−PPS20 (for details, see the caption of Figure 5). Inset d: normalized distribution of the longitudinal spread (for details, see the caption of Figure 7).

dimension actually ensures large polymer coating preventing or, at least minimizing nanotube−nanotube aggregating interactions. Also in this case we must remark the peculiar role of sulfide groups and, in particular, of methyl groups which dominate the tail at high value of the abscissa.

Similar to the model system, the effect of methyl and sulfide groups can be also appreciated from the higher value of CA found in correspondence of PEG44−PPS20 (10.5 ± 0.3 nm^2) with respect to the value for PEG44 (6.8 ± 0.2 nm^2) and reported in Figure S6 of the Supporting Information. This latter result, combined with the occurrence of interstitial water at the interface (very similar to the one shown by the model system) provides the density of inserted water molecules reported in Figure 12 together with the values referring to the model systems and previously cited through the text.

As expected, the combined action of chain dimension and chain density (i.e., the presence of PPS) produces a substantial dehydration of the interface. In this respect we can speculatively hypothesize that the interstitial water density tends to zero with the progressive increase of the dimensions of the chains and/or

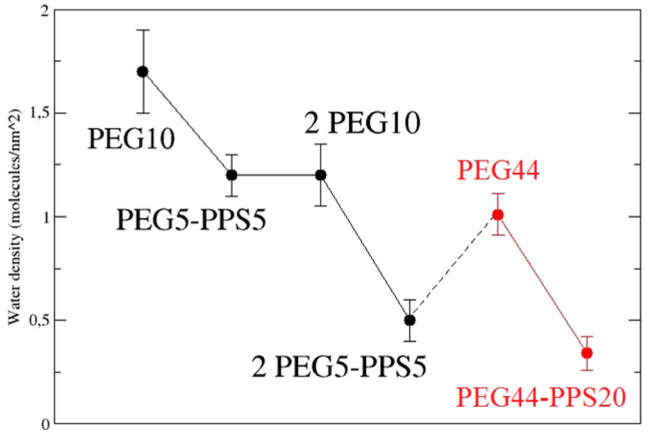

Figure 12. Density of interstitial water molecules and degree of hydration at the SWCNT-polymer interface for all the investigated systems.

dx.doi.org/10.1021/ma301534k | Macromolecules 2012, 45, 8043−8050

the presence of large number of polymer chains of block copolymer.

4. EXPERIMENTAL EVIDENCE

PEG44−PPS20 demonstrated[12] to be perfectly able to solubilize and disperse SWCNTs. Actually, experimental data evidenced that the solubilization apparently requires a concentration above the critical micellar concentration. In good agreement with the MD simulations, we can say that the solubilization requires instead the highest possible coverage of the SWCNT surface (see Discussion and Conclusions). In particular, PEG44−PPS20 proved to be the best dispersing diblock copolymer among the ones investigated in terms of dispersing ratio (weight of CNT to polymer). We checked the dispersing ability of PEG homopolymers of different lenghts but they did not show any capacity to disperse SWCNTs (Figure S7, Supporting Information) independent of their length (Table S2. Supporting Information).

5. DISCUSSION AND CONCLUSIONS

The use of computational-theoretical methods for describing a physically coherent and quantitatively predicting picture of SWCNT solubility through polymer chains is far beyond the possibilities of any currently available methodologies. However less general information can be realistically obtained with the currently available computational methodologies. In this study, by means of MD simulations, we have focused our attention on the hydrated polymer-SWCNT system concentrating on the morphological and mechanical analogies and differences between the homopolymer PEG and the diblock copolymer PEG−PPS, also considering the role of self-aggregating interactions, of polymer mass and of the solvent.

Recent experimental observations[12] have shown that a good SWCNT dispersion occurs with PEG−PPS concentrations well above the block copolymers critical aggregate concentration (CAC) and it has been also demonstrated that the driving force for the dispersion of SWCNTs is not the presence of micelles in solution, but rather the achievement of a good degree of SWCNT surface coverage. Also the accepted model for steric stabilization[14] does not necessarily implies the presence of micelles and is described as an essentially kinetically driven adsorption of one of the blocks of the block copolymer onto the nanotube surface, serving as the anchor, while the hydrophilic block extends and swells in the aqueous domain, imparting steric stabilization to the nanotube dispersion.[16] Similar conclusions were previously proposed by other investigators[52] who demonstrated that the ability of block copolymers to disperse carbon nanotube in water depends mainly on the interfacial tension parameter between the hydrophobic domain and the carbon nanotube (characterizing the difference between the adhesive energy between the nanotube and the hydrophobic block and the cohesive energy among the nanotubes).

The picture emerged by the present theoretical-computational study is not in disagreement with the above models. Analogies and differences with the proposed models have been found.

Our results, whose nature is essentially comparative and not absolute as they are based on the differences in some observables induced by the presence or absence of the PPS domain, can be briefly summarized as follows:

(i) Although no evidence arise from our study about the positive effect of PPS for enhancing the affinity toward SWCNT, the hydrophobic nature of PPS systematically ensures a higher SWCNT surface coverage that allows for weaker intertube contacts and makes phase separation more difficult, a higher interstitial water depletion, a much lower degree of water ordering;

(ii) On the contrary, the spread of the polymer in terms of normalized distribution of the longitudinal distance (Figure 11) is particularly high for PEG chains and recalls the spread of BSA on adsorption onto a graphite surface.[53] It is also worth noting that PEG chains tend to adopt a parallel arrangement of strands usually in the direction of the tube axis. We cannot explain this behavior but it is certainly due to interstrand interactions (dipolar and dispersion interactions) and is, as well, reminiscent of the predicted conformation of proteins on graphite.[54]

(iii) From our data, it is plausible, although not certain, that the presence of adsorbed aggregated chains onto the SWCNT surface, might amplify the affinity toward SWCNTs;

(iv) On the other hand, in none of our simulations have we observed hydrophilic chains extending and swelling in the aqueous domain, and hence, the analogy with the PPS serving as an anchor has not been proved by our simulations. Nevertheless, it is important to highlight that, in the present study, the available SWCNT surface was always higher than the potential coverage area of the polymer and we cannot exclude that dangling of the PEG chains onto the aqueous phase is the result of shortage of SWCNT surface;

(v) Much of the positive effects have been shown to be mainly due to the presence of the methyl and sulfide groups. Hence, it is possible that inclusion of longer alkyl moieties in the hydrophobic chain might induce significant changes in the dispersant ability.

■ ASSOCIATED CONTENT

Supporting Information

Analysis of the root mean square fluctuation for model systems, essential dynamics for model systems and extended systems, figures showing results for the root mean square fluctuation, spectrum of the eigenvalues of the all-atoms covariance matrix diagonalization, projection of the trajectories onto the essential plane, distribution of the number of water molecules found between the SWCNT surface and the adsorbed polymers along the MD simulations, RMSF of PEG44 and PEG44−PPS20, normalized distribution of the coverage area evaluated along the simulations, dispersion of 1 mg of SWCNT in 5 mL of 7 mg/mL aqueous solution of PEG34 and PEG90, tables of minimum distances of chain−nanotubes and dispersion of 1 mg of SWCNT in 5 mL of aqueous solution of homopolymer of different length. This material is available free of charge via the Internet at http://pubs.acs.org.

■ AUTHOR INFORMATION

Corresponding Author

*E-mail: m.aschi@caspur.it.

Notes

The authors declare no competing financial interest.

■ ACKNOWLEDGMENTS

The authors wish to acknowledge financial support by MIUR (PRIN 2008 – prot. 20085M27SS). This work was partly funded by CINECA-ISCRA (Italy) project C "Theoretical Modelling of Electron Transfer Reactions in Biomolecular Systems."

■ REFERENCES

(1) Liu, Z.; Tabakman, S.; Welsher, K.; Dai, H. *Nano Res.* **2009**, *2*, 85−120.
(2) De La Zerda, A.; Zavaleta, C.; Keren, S.; Vaithilingam, S.; Bodapati, S.; Liu, Z.; Levi, J.; Smith, B. R.; Ma, T.-J.; Oralkan, O.; Cheng, Z.; Chen, X.; Dai, H.; Khuri-Yakub, B. T.; Gambhir, S. S. *Nat. Nano.* **2008**, *3*, 557−562.
(3) Cherukuri, P.; Bachilo, S. M.; Litovsky, S. H.; Weisman, R. B. *J. Am. Chem. Soc.* **2004**, *126*, 15638−15639.
(4) Welsher, K.; Liu, Z.; Daranciang, D.; Dai, H. *Nano Lett.* **2008**, *8*, 586−590.
(5) Zavaleta, C.; de la Zerda, A.; Liu, Z.; Keren, S.; Cheng, Z.; Schipper, M.; Chen, X.; Dai, H.; Gambhir, S. S. *Nano Lett.* **2008**, *8*, 2800−2805.
(6) Liu, Z.; Sun, X.; Nakayama-Ratchford, N.; Dai, H. *ACS Nano* **2007**, *1*, 50−56.
(7) Kam, N. W. S.; O'Connell, M.; Wisdom, J. A.; Dai, H. *P. Natl. Acad. Sci. USA* **2005**, *102*, 11600−11605.
(8) Liu, Y.; Wu, D.-C.; Zhang, W.-D.; Jiang, X.; He, C.-B.; Chung, T. S.; Goh, S. H.; Leong, K. W. *Angew. Chem., Int. Ed.* **2005**, *44*, 4782−4785.
(9) Liu, Z.; Winters, M.; Holodniy, M.; Dai, H. *Angew. Chem., Int. Ed.* **2007**, *46*, 2023−2027.
(10) Bianco, A.; Kostarelos, K.; Prato, M. *Curr. Opin. Chem. Biol.* **2005**, *9*, 674−679.
(11) Di Crescenzo, A.; Velluto, D.; Hubbell, J. A.; Fontana, A. *Nanoscale* **2011**, *3*, 925−928.
(12) Di Meo, E. M.; Di Crescenzo, A.; Velluto, D.; O'Neil, C. P.; Demurtas, D.; Hubbell, J. A.; Fontana, A. *Macromolecules* **2010**, *43*, 3429−3437.
(13) Napper, D. H. *Polymeric Stabilization of Colloidal Dispersions*; Academic Press, Inc.: Orlando, FL, 1993.
(14) Shvartzman-Cohen, R.; Levi-Kalisman, Y.; Nativ-Roth, E.; Yerushalmi-Rozen, R. *Langmuir* **2004**, *20*, 6085−6088.
(15) Liu, X.; Tao, H.; Yang, K.; Zhang, S.; Lee, S.-T.; Liu, Z. *Biomaterials* **2011**, *32*, 144−151.
(16) Evans, D. F.; Wennersrom, H. *The colloidal domain where physics, chemistry, biology, and technology meet*, 2nd ed.; Wiley-VCH: New York, 1999.
(17) Nakashima, N. *Sci. Technol. Adv. Mater.* **2006**, *7*, 609−616.
(18) Woods, L. M.; Bădescu, Ş. C.; Reinecke, T. L. *Phys. Rev. B* **2007**, *75*, 155415.
(19) Belmares, M.; Blanco, M.; Goddard, W. A.; Ross, R. B.; Caldwell, G.; Chou, S. H.; Pham, J.; Olofson, P. M.; Thomas, C. *J. Comput. Chem.* **2004**, *25*, 1814−1826.
(20) Maurer, R. J.; Sax, A. F. *Phys. Chem. Chem. Phys.* **2010**, *12*, 9893−9899.
(21) Yang, M.; Koutsos, V.; Zaiser, M. *J. Phys. Chem. B* **2005**, *109*, 10009−10014.
(22) Duan, H.; Ding, F.; Rosén, A.; Harutyunyan, A.; Tokune, T.; Curtarolo, S.; Bolton, K. *Eur. Phys. J. D* **2007**, *43*, 185−189.
(23) Liu, Y.; Chipot, C.; Shao, X.; Cai, W. *J. Phys. Chem. C* **2011**, *115*, 1851−1856.
(24) Grujicic, M.; Cao, G.; Roy, W. N. *Appl. Surf. Sci.* **2004**, *227*, 349−363.
(25) Dalton, A. B.; Blau, W. J.; Chambers, G.; Coleman, J. N.; Henderson, K.; Lefrant, S.; McCarthy, B.; Stephan, C.; Byrne, H. *Synth. Met.* **2001**, *121*, 1217−1218.
(26) Chiu, C.-c.; Maher, M. C.; Dieckmann, G. R.; Nielsen, S. O. *ACS Nano* **2010**, *4*, 2539−2546.
(27) Chiu, C.-c.; Dieckmann, G. R.; Nielsen, S. O. *Peptide Sci.* **2009**, *92*, 156−163.
(28) Yang, S.-H.; Cheng, Y.-K.; Yuan, S.-L. *J. Mol. Model.* **2010**, *16*, 1819−1824.
(29) Johnson, R. R.; Johnson, A. T. C.; Klein, M. L. *Nano Lett.* **2007**, *8*, 69−75.
(30) Tang, L.; Yang, X. *J. Phys. Chem. C* **2012**, *116*, 11783−11791.
(31) Enyashin, A. N.; Gemming, S.; Seifert, G. *Nanotechnology* **2007**, *18*, 245702.
(32) Gowtham, S.; Scheicher, R. H.; Pandey, R.; Karna, S. P.; Ahuja, R. *Nanotechnology* **2008**, *19*, 125701.
(33) Srinivas, G.; Klein, M. L. *Nanotechnology* **2007**, *18*, 205703.
(34) Wallace, E. J.; Sansom, M. S. P. *Nano Lett.* **2007**, *7*, 1923−1928.
(35) Wallace, E. J.; Sansom, M. S. P. *Nanotechnology* **2009**, *20*, 045101.
(36) Gurevitch, I.; Srebnik, S. *J. Chem. Phys.* **2008**, *128*, 144901−144908.
(37) Johnson, R. R.; Rego, B. J.; Johnson, A. T. C.; Klein, M. L. *J. Phys. Chem. B* **2009**, *113*, 11589−11593.
(38) White, C. T.; Robertson, D. H.; Mintmire, J. W. *Phys. Rev. B* **1993**, *47*, 5485−5488.
(39) Berendsen, H. J. C.; Postma, J. P. M.; van Gunsteren, W. F.; Di Nola, A.; Haak, J. R. *J. Chem. Phys.* **1984**, *81*, 3684−3690.
(40) Darden, T.; York, D.; Pedersen, L. *J. Chem. Phys.* **1993**, *98*, 10089−10092.
(41) Lindahl, E.; Hess, B.; van der Spoel, D. *J. Mol. Model.* **2001**, *7*, 306−317.
(42) Lee, H.; Venable, R. M.; MacKerell, A. D., Jr.; Pastor, R. W. *Biophys. J.* **2008**, *95*, 1590−1599.
(43) Oostenbrink, C.; Villa, A.; Mark, A. E.; Van Gunsteren, W. F. *J. Comput. Chem.* **2004**, *25*, 1656−1676.
(44) Berendsen, H. J. C.; Postma; J. P. M.; van Gunsteren, W. F.; Hermans, J. Interaction models for water in relation to protein hydration. In *Intermolecular forces*; Pullman, B., Ed.; D Reidel Publishing Company: Dordrecht, The Netherlands, 1981; pp 331−342.
(45) Cerritelli, S.; O'Neil, C. P.; Velluto, D.; Fontana, A.; Adrian, M.; Dubochet, J.; Hubbell, J. A. *Langmuir* **2009**, *25*, 11328−11335.
(46) Cerritelli, S.; Fontana, A.; Velluto, D.; Adrian, M.; Dubochet, J.; De Maria, P.; Hubbell, J. A. *Macromolecules* **2005**, *38*, 7845−7851.
(47) Azri, A.; Giamarchi, P.; Grohens, Y.; Olier, R.; Privat, M. *J. Colloid Interface Sci.* **2012**, *379*, 14−19.
(48) Amadei, A.; Linssen, A. B. M.; Berendsen, H. J. C. *Proteins: Struct. Funct. Genet.* **1993**, *17*, 412−425.
(49) Xie, Y. H.; Soh, A. K. *Mater. Lett.* **2005**, *59*, 971−975.
(50) Pang, J.; Xu, G.; Tan, Y.; He, F. *Colloid Polym. Sci.* **2010**, *288*, 1665−1675.
(51) Friling, S. R.; Notman, R.; Walsh, T. R. *Nanoscale* **2010**, *2*, 98−106.
(52) Nagarajan, R.; Bradley, R. A.; Nair, B. R. *J. Chem. Phys.* **2009**, *131*, 104906−104913.
(53) Mücksch, C.; Urbassek, H. M. *Langmuir* **2011**, *27*, 12938−12943.
(54) Raffaini, G.; Ganazzoli, F. *J. Phys. Chem. B* **2004**, *108*, 13850−13854.